Proceedings of the 39th IAHR World Congress
19-24 June 2022
Granada, Spain
DOI number

Transport and Capture of Neutrally Buoyant Particles in Streams: Investigating the Effect of Obstacle Configuration

Hojung You[1] and Rafael O. Tinoco [2]

[1,2] Department of Civil Engineering, University of Illinois at Urbana-Champaign, Il, USA
hojungy2@illinois.edu
tinoco@illinois.edu

Abstract

The transport of particles in water is a mechanism observed from various scientific and engineering problems such as the removal of polluted particles, optimal sampling of organic matter, transport of fish eggs and plant seeds. Thus, it is necessary to understand the transport mechanism of particulate matter in water thoroughly to manage the aquatic ecosystem effectively. In this study, we analyze the transport of neutrally buoyant particles in a laboratory setting when obstacles are fixed at the bottom with different configurations, focusing on the spacing between neighboring obstacles at different flow depths and velocities. The spatial and temporal analysis of two-dimensional velocity fields yield valuable information on flow-structure-particle interactions and their response to changing hydrodynamic conditions. We conducted experiments on a closed-loop racetrack flume, using Particle Tracking Velocimetry (PTV) to identify plastic transport and their preferred locations relative to the obstruction, and Particle Image Velocimetry (PIV) to identify specific mean and turbulent conditions that determine particle retention or redirection. Based on the result, we computed two parameters, the dimensionless capture ratio and retention time of particles to quantify the effect of submerged obstructions on the transport of particles. Spectrum analysis and quadrant analysis are applied to show that large scale eddies appear at the threshold gap length and lead to high concentration of particles inside the gap between adjacent obstacles, creating a favorable condition to capture particles effectively.

Keywords: Particle transport; Particle Image Velocimetry (PIV); Particle Tracking Velocimetry (PTV), Invasive species, Microplastics

1. INTRODUCTION

Freshwater transports various types of particulate matters including fish eggs, plant seeds, invertebrates and microplastics (Prada et al., 2021; Shi et al., 2021; McQueen et al., 2020). Particles such as microplastics and invasive eggs and seeds can cause detrimental effect on the ecosystem when they are excessively accumulated or advected to unexpected regions. On the other hand, some particles such as invertebrates and eggs of native species need to be successfully transported to maintain the present ecosystem. Thus, it is necessary to understand the transport mechanism of such particulate matter in freshwater to develop an efficient management strategy of the aquatic ecosystem (Hoellein et al., 2014). Common obstacles in freshwater such as branches, logs and hydraulic structures, are identified as local hotspots of particles of different sizes, shapes and densities (Martin et al., 2019; Kapp and Yeatman 2018). Hydrodynamic analysis of these locations can provide a more efficient approach to predict the concentration of particles that develop around typical geometries found in freshwater ecosystems.

While previous studies suggest that particles are commonly trapped by obstacles in water, we still lack understanding of how particle transport is actually affected by the presence of such obstacles. A proper analysis requires focusing on the mean and turbulent hydrodynamic changes due to obstacles, and the resulting interactions between flow and particulate matters. In this study, we analyze the transport of particles based on surrounding flow characteristics by conducting simplified two-dimensional laboratory experiments with two submerged obstacles under uni-directional flows. Results from our study can be used to: 1) predict the accumulation zone of particles for monitoring or their redirection in streams, and 2) design artificial traps to target specific particulate matter without affecting transport of desirable stream organisms.

2. METHODS

Experiments were conducted at the uni-directional and recirculating Odell-Kovasznay flume at the Ecohydraulics and Ecomorphodynamics Laboratory at the University of Illinois at Urbana-Champaign. The test

section of the flume is 2 m long, 0.15 wide, and water depth was maintained as *H* = 0.2 ~ 0.4 m. Two rectangular obstacles with 0.04 m length, 0.15 m width and *h* = 0.1 m height, made of Lego blocks were installed at the bottom of the flume. These obstacles resemble generic submerged matter in actual environments, such as vegetation, artificial structures or sunk materials. Three variables are included in this study. (1) Distance between two obstacles, *d*, which varied from 0.04 to 0.4 m, with increments of *L* = 0.04 m, where *L* is the length of the obstacle. (2) Flow depth, *H*, varying from 0.1 to 0.45 m. (3) Flow velocity ranging between 0.12 ~ 0.24 m/s. Flow velocity remained consistent throughout each experiment condition by setting the rotating disc-pump frequency at a fixed value. Dimensionless parameters computed based on experiment conditions prove that flow is fully turbulent and sub-critical. Fluorescent Green Polyethylene microspheres (Cospheric, UVPMS-BG-1.00) were used in our experiments, chosen for their circular shape with neutrally buoyant density, and 1 mm diameter.

Particle trajectories were recorded after dropping particles into the water and waiting for few minutes so that particle distributions are uniform in longitudinal, lateral and vertical directions. Particle trajectories were recorded for 60 seconds with a 5-Megapixel CCD camera (JAI GO-5000M-USB3, 2560 × 2048 pixels, 50 frames per second), installed to the side of the test section. Two black light lamps were placed at the top of the flume to clearly visualize the motion of fluorescent particles. Recordings were processed using a custom particle image processing Matlab routine to obtain particle trajectories based on a two-step process: 1) particle identification from each frame, and 2) particle matching between two consecutive frames (Brevis et al., 2011).

Images for 2D analysis of flow fields were obtained using an Edgertronic SC2 high-speed camera (1280 × 864 pixels, 100 frames per second) located at the side of the flume. Recording lasted for 60 seconds and images were processed using PIVlab, a Matlab-based toolbox (Thielicke and Stamhuis, 2014). A 5W continuous-wave laser, located at the top of the flume, generated a planar light sheet at the centerline of the flume (Figure 1).

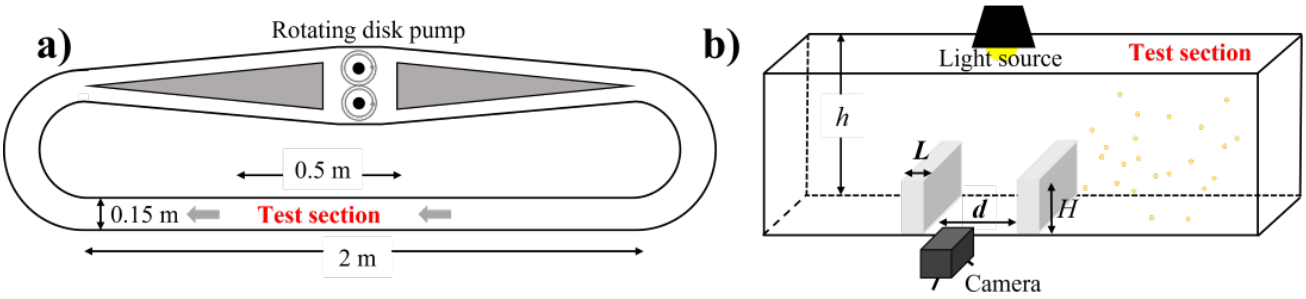

Figure 1. a) Top-view of Odell-Kovasznay flume. b) Side-view of test section with the experimental setup.

Based on full trajectories of every particle obtained from PTV, the efficiency of particle capture in between two obstacles was quantified by computing normalized capture ratio and retention time. Normalized capture ratio C_p was computed as Eq. [1]:

$$C_p = \frac{1}{d}\frac{N_c}{N} \quad [1]$$

where d is the distance between two obstacles, N is the total number of particles passing by the upstream obstacle and N_c is the number of captured particles in between the gap. Retention time was computed by counting the number of frames that each particle took to pass both upstream and downstream obstacles.

Instantaneous velocity fields were averaged over time to compute $\bar{u}(x,z)$ and $\bar{w}(x,z)$. Turbulent fluctuations were obtained by Reynolds decomposition as $u'(x,z) = u(x,z) - \bar{u}(x,z)$ and $w'(x,z) = w(x,z) - \bar{w}(x,z)$. The power spectral density was computed by a Fourier transform of the vertical velocity fluctuation as Eq. [2]:

$$E(f) = \int_{-\infty}^{\infty} |w'(t)|^2 \, dt \quad [2]$$

Quadrant analysis was performed based on the turbulent fluctuations to analyze the occurrence of four turbulent events, which are: 1) outward interaction ($u' > 0$, $w' > 0$, Quadrant 1), ejection ($u' < 0$, $w' > 0$, Quadrant 2), inward interaction ($u' < 0$, $w' < 0$, Quadrant 3) and sweep ($u' > 0$, $w' < 0$, Quadrant 4).

3. RESULTS AND DISCUSSION

3.1 The Capture Efficiency Inside the Gap Between Two Obstacles

Particle trajectories, obtained as composite images for 1 minute of data (Figure 2a-c) and vorticity contours from PIV data (Figure 2d-f) for three spacing cases (*d*/*L* = 2, 5 and 9), reveal a clear retention pattern. The shapes of particle trajectories were different for all three spacing conditions, showing that particle behaviors are dependent on the flow structures generated in between the gap of obstacles. At short spacing condition, *d*/*L* = 2, particles showed random behaviors rather than having coherent trajectories, while a clear circular shape of trajectories emerged at a spacing of *d*/*L* = 5, which indicates that particles were captured in large rotating eddies inside the gap. This implies that there is a critical value of obstacle spacing to generate strong flow structures and influence particle motions in general. When the spacing was further increased to *d*/*L* = 9, different particle behaviors were observed, and the circular shape of particle trajectories leaned toward the downstream obstacle, while random particle behaviors were observed close to the upstream obstacle. Comparing the shape of particle trajectories with vorticity contours, the vertical rotating motion of particles are clearly driven by high vorticities generated after spacing larger than *d*/*L* = 5.

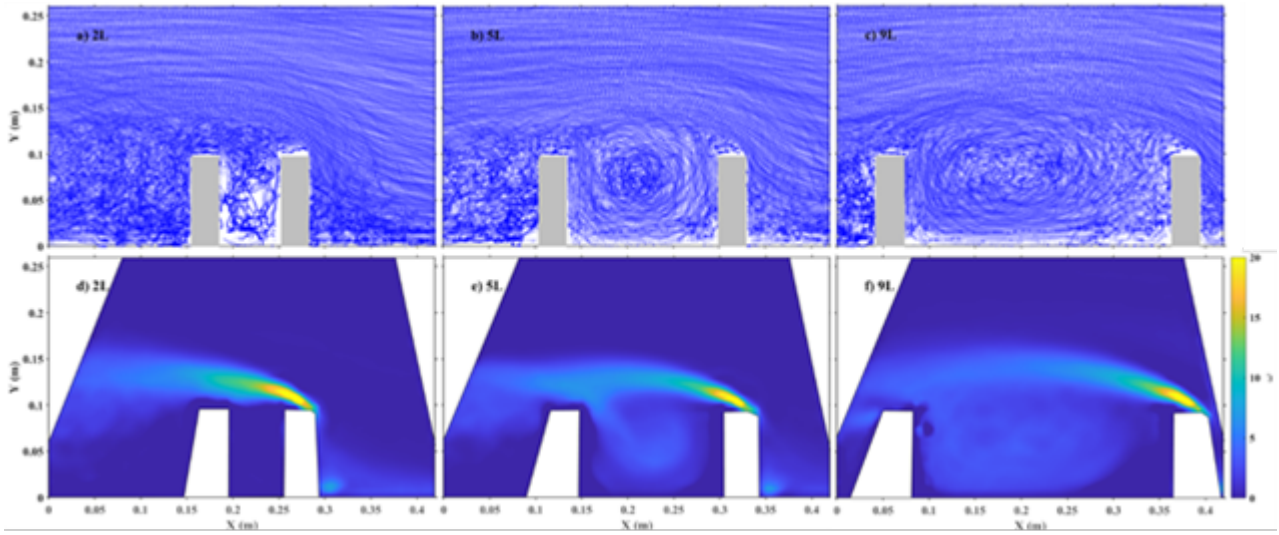

Figure 2. Particle trajectories during 1 min for a) *d*/*L* = 2, b) *d*/*L* = 5, c) *d*/*L* = 9 and vorticity contours for d) *d*/*L* = 2 e) *d*/*L* = 5 f) *d*/*L* =9 at fixed flow depth *h* = 0.3 m and mean velocity *U* = 0.175 m/s

We calculated indices of particle capture efficiency (Figure 3). C_p, as defined in Eq. [1], is the normalized capture ratio and T_r is the retention time of particles, which is computed for both captured and non-captured particles. As spacing increased, the normalized capture ratio increased until *d*/*L* = 5 and later converged to a consistent value. In Figure 2, *d*/*L* = 5 was the critical distance that led particles to circulate in between the gap. Until *d*/*L* = 5, increasing the spacing led flow structures to develop and increased normalized capture ratio. However, once circular flow structures were fully established, further increasing the distance and growth of an eddy size did not affect the normalized capture ratio. Retention time of particles is another indicator of particle capture efficiency. It was expected that retention time would increase with *d*/*L*, since it would take longer to move longer distances. Such an increase was observed for particles that were bypassing the obstacles without being entrapped, which are illustrated by red markers in Figure 3b, showing a linear increasing trend in response to linearly increasing distance. However, retention time of captured particles, presented with blue marker on Figure 3b, had a different trend, which decreased at short spacing range (*d*/*L* = 1 ~ 3) and converged at long spacing range (*d*/*L* = 7 ~ 10).

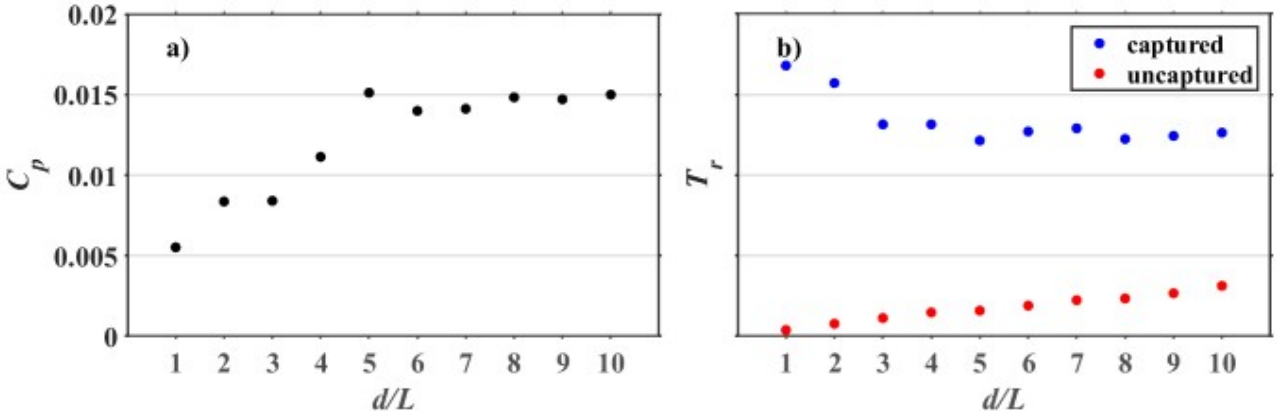

Figure 3. Quantification of particle capture efficiency between two obstacles at different gap lengths: a) normalized capture ratio, b) retention time of captured and uncaptured particles.

Dimensionless capture ratio and retention time of particles were computed at various flow depth and flow velocities, and results are provided in Figure 4. The first-increasing and then-converging trend of C_p was commonly observed at various flow conditions when *d*/*L* increased. Data showed that the transport of particles is dependent on the flow conditions, with C_p increasing at faster flow velocities and lower flow depths. On the contrary, T_r of captured particles showed decreasing and later-convering trends at majorities of flow conditinos when *d*/*L* increased. T_r decreased at faster velocities and lower flow depths.

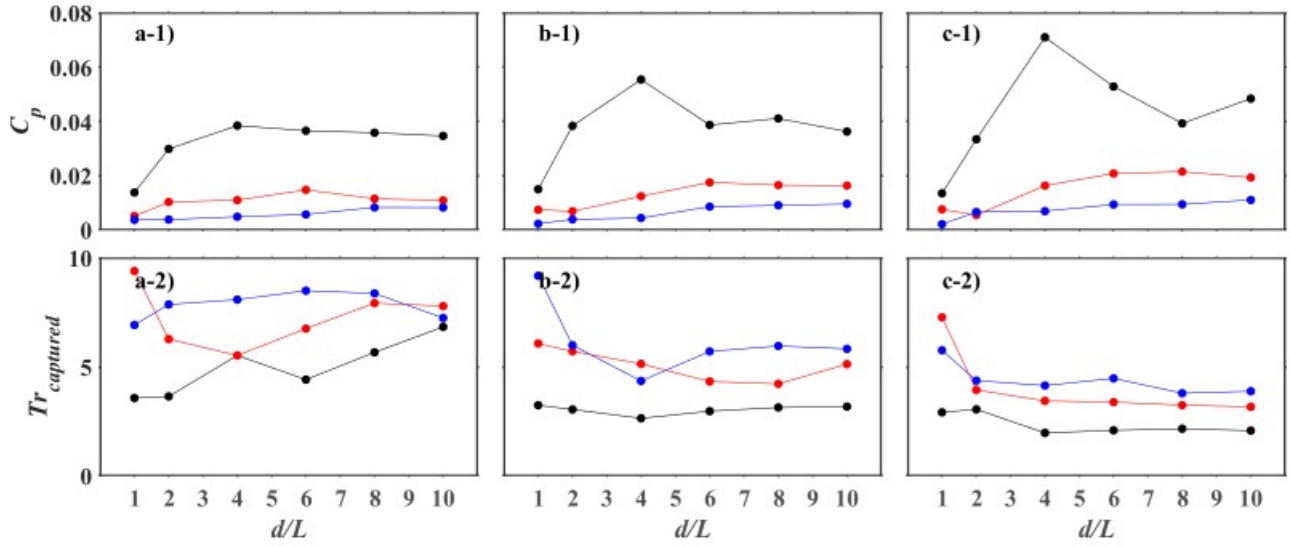

Figure 4. Quantification of particle capture efficiency between two obstacles at different gap lengths, flow depth and flow velocities: a) *f* = 20 Hz (0.117 m/s), b) *f* = 30 Hz (0.175 m/s), c) *f* = 40 Hz (0.232 m/s). ●: *h*/*H* = 2, ●: *h*/*H* = 3, ●: *h*/*H* = 4.

3.2 The Evolution of Flow Structures and Their Effect on Particle Behaviors

Compared to the broad band spectral distribution at small gap length (Figure 5a), a distinctive peak of the frequency spectrum in Figure 5c (corresponding to *d*/*L* = 5) suggests energy-containing eddies have developed at the gap between two obstacles. The peak occurs roughly at $f \approx 1Hz$. Considering that *U* = 0.175 m/s, the eddy size can be approximated as $L_e \approx 0.175m$, which is equivalent to the distance between two obstacles at *d*/*L* = 5. The highest capture ratio at *d*/*L* = 5 indicates that the gap length should be large enough to create an eddy that leads to higher entrainment of particles inside the gap. Once the eddy is developed, increasing the gap length did not increase the capture ratio, indicating that the existence of these eddies is the most significant factor to create a condition to capture particles effectively.

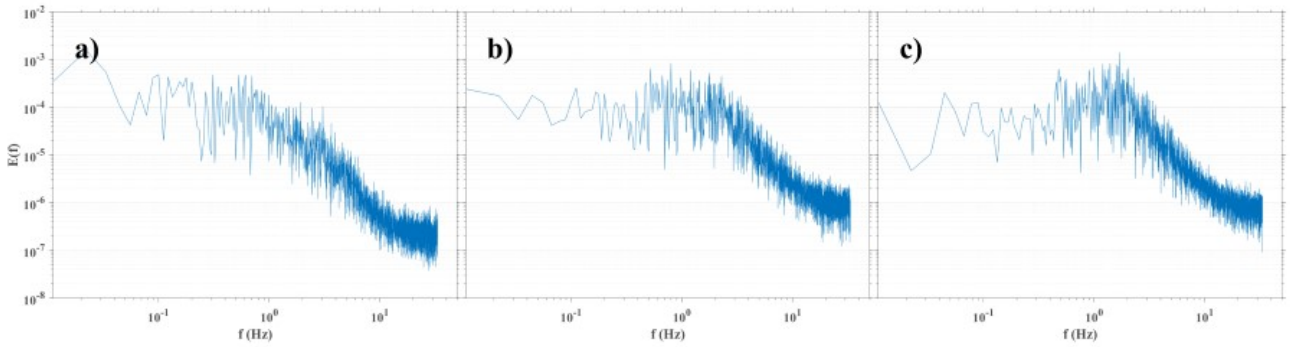

Figure 5. Turbulence energy spectra at the center of the gap between two obstacles: a) *d*/*L* = 1, b) *d*/*L* = 4, c) *d*/*L* = 5.

The uneven distribution of turbulent fluctuations observed from the quadrant analysis represents the anisotropic turbulence field. The dominance of sweep and ejection events occurs from the coherent structures developed between the two obstacles. The shear layer is specifically dominated by ejections, which arise from the damped flow coupled with increased turbulence fluctuations. This retards the particle motion passing above the obstacles, which increases the possibility of particles being captured in between the gap. Dominance of sweeps due to accelerating and descending fluid motion also increases the penetration of outer flow into the gap, contributing to the active entrainment of particles.

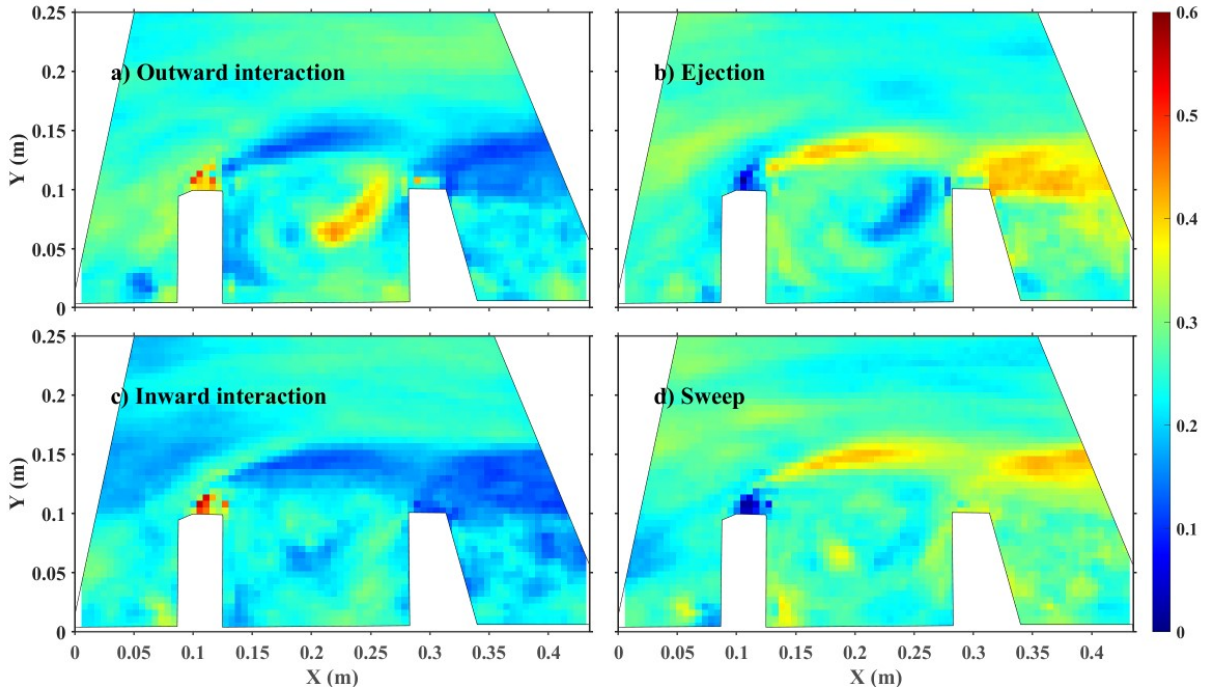

Figure 6. The ratio of turbulent events at *d*/*L* = 5: a) outward interaction (Q1), b) ejection (Q2), c) inward interaction (Q3) and d) sweep (Q4).

4. CONCLUSIONS

We present two indices of particle capture efficiency in this study: normalized capture ratio and retention time. Their values in response to spacing between two obstacles imply that there is a threshold to determine the most efficient length to capture particles inside the gap (identified as 5*L* for this study, where *L* is the length of the obstacle). Particle motions were dependent on flow structures. In particular, vorticity was related to a circular rotating motion of particles within the gap. It is expected that findings of our current study could be applied to future management strategies by providing effective monitoring, sampling, and capture strategies for invasive eggs and drifting particle, as well as guidelines for the designing of novel species-targeted traps.

5. ACKNOWLEDGEMENTS

This material is based upon work supported by the U.S. Geological Survey under Grant G22AP00022. Any use of trade, firm, or product names is for descriptive purposes only and does not imply endorsement by the U.S. Government.

6. REFERENCES

Brevis, W., Niño, Y., & Jirka, G. H. (2011). Integrating cross-correlation and relaxation algorithms for particle tracking velocimetry. *Experiments in Fluids*, *50*(1), 135-147.

Hoellein, T., Rojas, M., Pink, A., Gasior, J., & Kelly, J. (2014). Anthropogenic litter in urban freshwater ecosystems: distribution and microbial interactions. *PloS one*, *9*(6), e98485.

Kapp, K. J., & Yeatman, E. (2018). Microplastic hotspots in the Snake and Lower Columbia rivers: A journey from the Greater Yellowstone Ecosystem to the Pacific Ocean. *Environmental Pollution*, *241*, 1082-1090.

Martin, C., Corona, E., Mahadik, G. A., & Duarte, C. M. (2019). Adhesion to coral surface as a potential sink for marine microplastics. *Environmental Pollution*, *255*, 113281.

McQueen, R., Ashmore, P., Millard, T., & Goeller, N. (2021). Bed particle displacements and morphological development in a wandering gravel-bed river. *Water Resources Research*, *57*(2), e2020WR027850.

Prada, A. F., George, A. E., Stahlschmidt, B. H., Jackson, P. R., Chapman, D. C., & Tinoco, R. O. (2021). Using turbulence to identify preferential areas for grass carp (*Ctenopharyngodon idella*) larvae in streams: a laboratory study. *Water Resources Research*, *57*(2), e2020WR028102.

Shi, W., Peruzzo, P., & Defina, A. (2021). An Eulerian model for the transport and diffusion of floating particles within regions of emergent vegetation. *Water Resources Research*, *57*(8), e2021WR029625.

Thielicke, W., & Stamhuis, E. (2014). PIVlab–towards user-friendly, affordable and accurate digital particle image velocimetry in MATLAB. *Journal of open research software*, *2*(1).